Cross-Domain Inference-Conditioned Interdiction in Coupled Fuel–Electric Power Networks

Ricardo Marquez, Ph.D.
rmarquez123@gmail.com

***Abstract*—Power-system N–k interdiction identifies the k component failures that maximize load curtailment, and is conventionally formulated over a fixed, single-domain electrical model. This paper examines whether inference that couples two conservation domains alters the interdiction decision when generation is limited by an upstream fuel-supply constraint rather than an electrical one. The analysis employs a domain-independent multi-conservation graph engine that assembles conservation residuals and their Jacobian from a declarative model and performs maximum-a-posteriori (MAP) estimation with a Laplace posterior covariance. On an IEEE 14-bus AC network augmented with a gas-fired generator whose availability is a free log-normal variable, coupled into the network as an equality injection, a single remote electrical measurement reduces the posterior standard deviation of the fuel-availability variable by 21.7% in the absence of any fuel telemetry. A control in which the same injection is fixed to a constant eliminates this effect, confirming that the coupling, rather than the estimator, is responsible. When the posterior is propagated to a minimum-load-shed interdiction, a biased fuel measurement is corrected by the electrical evidence (available capacity 265 to 210 MW; true value 120 MW). The joint estimate is 90 MW closer to the true reserve than the sequential estimate and halves the mean interdiction regret against the true-state optimum (8.2 versus 17.9 MW). On this capacity-rich network the change in the selected interdiction is confined to a narrow stress band, which is explained by a transmission-congestion mechanism that caps the usable reserve. The contribution is a capability: cross-domain coupled inference obtained directly from a declarative model, which a fixed-scenario, single-domain workflow does not provide.**

***Index Terms*—Power system interdiction, N–k security, state estimation, multi-energy systems, infrastructure interdependencies, Bayesian inference.**

I. Introduction

Critical infrastructures do not fail one domain at a time. Electric power, natural gas, and their controls are interdependent, and a disturbance in one propagates into the others [1]. The standard formulation for adversarial grid security, N–k interdiction, selects the k component removals that maximize disruption [2], [3] and is posed over a fixed, purely electrical model, in some variants with a probability distribution over failures [4], [5]. When the binding constraint is a fuel limit rather than an electrical one, the electrical telemetry available to operators carries information about the fuel state, and a single-domain formulation cannot exploit it.

This coupling is operationally significant. Gas-fired generation supplies a large and growing share of electric energy, and its output can be curtailed by fuel-delivery constraints that originate outside the electrical network [6]; during correlated stress events such as cold snaps, the gas and electric systems have historically failed together [1]. At the same time, operators observe the electrical network densely—voltages, flows, and injections—but the fuel-supply state only sparsely. A security assessment that treats generator capacity as a fixed input therefore discards information that the electrical measurements contain about fuel availability, and may misrank the critical contingencies. The practical question is whether that discarded information is sufficient to change a decision, not merely to refine an estimate.

Accordingly, this paper addresses the following question: can inference that couples two conservation domains alter an interdiction decision that a per-domain estimator cannot? The question is examined on a concrete, fully reproducible instance, and the result is reported both where it is strong and where it is limited.

The contributions are as follows. First, a coupling construction and a separability criterion (Proposition 1, Section IV) under which the fuel and electrical states are non-separable, with a one-line control that removes the coupling. Second, an inference-level result (Section V): a remote electrical measurement informs the fuel state, robustly across measurement noise, sensor placement, and sensor count. Third, a decision-level result (Section VI): the coupled posterior lowers the interdiction regret against the true-state optimum, and where it changes the selected interdiction the narrowness is explained by a transmission-congestion mechanism.

II. Related work

Power-grid interdiction originates with the bilevel min-max formulation of Salmeron, Wood, and Baldick [2] and the N–k models of Bienstock and Verma [3]; Sundar *et al.* add a probabilistic failure distribution and stochastic variants [4], [5]. All of these fix a single-domain electrical model and treat generator capacity as given. Multi-energy coupling is studied separately: the "energy hub" optimal power flow of Geidl and Andersson couples gas and electricity through conversion efficiencies [6], and infrastructure-interdependence analysis characterizes cross-domain propagation qualitatively [1]. Power-system

state estimation is a mature weighted-least-squares discipline [7], [8], and the Laplace approximation provides its posterior covariance [9]. The present work sits at the intersection: it uses coupled cross-domain *inference* to condition an interdiction decision, rather than coupling the domains only in the deterministic model or treating estimation and interdiction as separate single-domain problems.

III. Preliminaries

A. N–k interdiction and the minimum-load-shed problem

An N–k interdiction chooses a set A of k components to remove so as to maximize the operator's best-case load shed. The inner problem considered here is the DC minimum-load-shed linear program: given the surviving network, generation is redispatched and the least load is shed consistent with DC power flow and generator limits [2], [3]. Denoting the resulting minimum shed by $Q(A)$, the interdiction is $\max_{|A|=k} Q(A)$; stochastic variants take an expectation of Q over a failure distribution [4], [5]. The quantity Q depends on each generator's available capacity $p_{\max}$. When $p_{\max}$ is set by fuel availability, the interdiction value depends on a fuel quantity that the electrical model treats as a fixed input. Coupling between energy carriers is well studied; the multi-energy "energy hub" optimal power flow couples gas and electricity through conversion efficiencies [6]. The present contribution is not a new coupled model, but a demonstration that coupled *inference* over such a model alters a security decision.

B. The multi-conservation graph engine

The analysis employs TERRA, a domain-independent multi-conservation graph engine. A model is specified as a graph in which nodes carry conservation laws—one balance per domain, here electrical active and reactive power and fuel mass—and edges carry the constitutive flows between them. From this specification the engine assembles a residual vector $r(z)$, with one entry per conservation law and closure, together with its analytic Jacobian $J = \partial r/\partial z$, and obtains the deterministic state by solving $r(z) = 0$ with Newton's method. For inference, measurements and priors are treated as a weighted-least-squares problem, and the MAP estimate

$$z^\star = \arg\min_z \tfrac{1}{2}\|r(z)\|^2_{\Omega_p} + \tfrac{1}{2}\|h(z) - y\|^2_{\Omega_y} \qquad (1)$$

is computed by Gauss–Newton using the same r and J [7], [8]. The Laplace approximation then yields the posterior covariance $\Sigma = \Lambda^{-1}$ from the information matrix $\Lambda = J^\top \Omega J$ [9]. The formulation is domain-independent: the residual, Jacobian, and information matrix do not distinguish an electrical balance from a fuel balance, so a single posterior spans both domains. This property is the subject of the present study.

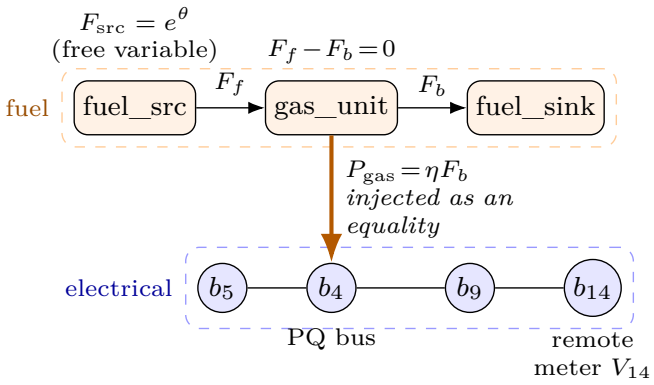


Fig. 1. The coupled multi-conservation graph. A three-node gas subsystem is attached to bus b_4 of the electrical network. Fuel availability $F_{\text{src}} = e^\theta$ is a single free variable, and its real-power injection $P_{\text{gas}} = \eta F_b$ enters the active-power balance of b_4 as an equality (a variable-valued source is a free flow in the conservation row), so θ appears inside an electrical residual. A remote measurement V_{14} therefore constrains the fuel variable through the AC power flow. Specifying the injection as a fixed scalar instead (the separable control) removes this path.

IV. The coupled model and separability

The model builds on the standard IEEE 14-bus AC network [10] with a gas-fired unit added at bus b_4 (a PQ, non-slack bus). The gas subsystem (Fig. 1) is a three-node fuel chain: a reservoir supplies fuel $F_f = k_f(F_{\text{src}} - P_f)$ to the unit, which burns it as $F_b = k_b P_f$, and fuel availability is log-normal, $F_{\text{src}} = e^\theta$, with θ the single free fuel degree of freedom. The unit's electrical injection is the conversion $P_{\text{gas}} = \eta F_b$.

The critical modeling choice concerns how P_{gas} enters the electrical model. It is injected into the active-power balance of b_4 as an equality; in the engine, a variable-valued source appears as a free flow in that conservation row:

$$\textstyle\sum_{\ell \in b_4} P_\ell(V, \delta) \;=\; P_{\text{gas}}(\theta), \qquad P_{\text{gas}} = \eta\, k_b\, P_f. \qquad (2)$$

Because (2) places θ inside an electrical residual, the information matrix is not block-diagonal between the fuel and electrical variables. This is made precise as follows.

Proposition 1. *Partition the free variables as $z = (z_f, z_e)$ into a fuel block (containing θ) and an electrical block, and let the weighting Ω be diagonal in the residual rows. The information matrix $\Lambda = J^\top \Omega J$ has a nonzero fuel–electrical block Λ_{fe} if and only if at least one residual row depends on both a fuel and an electrical variable. Under the equality coupling (2), $\Lambda_{fe} \neq 0$; if the injection is instead a fixed scalar, θ enters no electrical residual and $\Lambda_{fe} = 0$.*

Proof. Writing r_k for the k-th residual, $\Lambda_{fe} = \sum_k \Omega_{kk}\,(\partial r_k/\partial z_f)(\partial r_k/\partial z_e)^\top$. A summand is nonzero only when $\partial r_k/\partial z_f \neq 0$ and $\partial r_k/\partial z_e \neq 0$, i.e. when row k depends on both blocks. The bus-4 active-power balance (2) depends on θ (through P_{gas}) and on the electrical state (V, δ), and is the only such row; it therefore populates Λ_{fe}.

TABLE I
Conditioning and non-separability gate (IEEE-14 AC, 120 free variables).

check	value	verdict
converges	MAP $\theta = -0.508$ (true -0.511)	GO
$\mathrm{cond}(\Lambda) \le 10^{10}$	3.56×10^7	GO
identifiable / Laplace	"well" / ESS 0.987	GO
$\mathrm{corr}(\theta, V_{14})$	0.224 (network-mediated)	GO
elec-only informs θ	std drop 21.7%	GO
separable control	std drop 0.0%, cov 0	GO
overall		**GO**

Replacing $P_{\mathrm{gas}}(\theta)$ by a constant removes θ from that row, emptying the set and giving $\Lambda_{fe} = 0$. □

Proposition 1 is verified directly with a separable control that replaces the variable injection in (2) by a fixed scalar, leaving the model otherwise unchanged: it must yield $\mathrm{cov}(\theta, V_{14}) = 0$.

V. Inference-level results

Soft priors are attached to the electrical state and a loose prior to θ (mean off-truth, standard deviation 0.800). The available measurements are a coarse fuel meter and three remote electrical meters (voltages at b_{14} and b_{13} and a line flow, all remote from b_4). Table I reports the pre-registered acceptance gate: the estimator converges, Λ is well-conditioned ($\mathrm{cond} = 3.56 \times 10^7 \le 10^{10}$), θ is identifiable with a valid Laplace posterior (effective-sample-size ratio 0.987), and the non-separability condition holds, $\mathrm{cov}(\theta, V_{14}) \neq 0$ with $\mathrm{corr} = 0.224$.

Fig. 2(a) presents the principal quantity. With remote electrical evidence alone and no fuel telemetry, the posterior standard deviation of θ falls from the prior value 0.800 to 0.627, a reduction of 21.7%; electrical data alone has informed a purely fuel quantity. The separable control, identical except for the fixed-scalar injection, leaves the standard deviation at 0.800 ($\mathrm{cov} = 0$). This establishes the inference-level result: cross-domain coupled inference is effective, and the coupling in (2), rather than an artifact of the estimator, is responsible.

The effect is robust to the measurement conditions (Table II). It degrades gracefully as the electrical-meter noise grows, and it persists as the sensor count is reduced. Sensor *placement* matters most: remote sensors (all far from the gas bus) give a 22% reduction in the θ standard deviation, while sensors adjacent to the gas bus give 92%. This is an operationally useful finding: instrumenting near a fuel-limited unit sharpens the estimate of its availability, but even remote instrumentation is informative through the network coupling.

VI. Decision-level results

The posterior is next propagated to an interdiction decision (Fig. 3). The gas unit at b_4 serves as a background reserve, and the interdiction candidates are the non-gas generators, so that the unit's inferred availability is decision-relevant. The fuel meter is coarse and biased high (bias +0.35, noise 0.6), over-reading the reserve. The sequential baseline estimates the reserve from fuel telemetry only and adopts the inflated value (265 MW), whereas the joint estimator corrects it downward using the remote electrical evidence (210 MW; true value 120 MW).

TABLE II
Sensitivity of the fuel-posterior reduction (electrical evidence only).

condition	θ std	reduction (%)
noise $\times 0.5$	0.481	40
noise $\times 1$	0.627	22
noise $\times 2$	0.721	10
noise $\times 4$	0.761	5
far	0.627	22
near	0.067	92
far+near	0.067	92
1 far sensors	0.667	17
2 far sensors	0.663	17
3 far sensors	0.627	22

TABLE III
Interdiction across load stress: the sequential and joint recommendations, the true-state optimum, and the regret (R, MW) of each recommendation against it.

load	$A^\star_{\mathrm{seq}}$	$A^\star_{\mathrm{joint}}$	$A^\star_{\mathrm{true}}$	R_{seq}	R_{joint}	stab.
3.3	g_3	g_3	g_2	30.3	30.3	y
3.4	g_3	g_3	g_2	35.7	35.7	n
3.5	g_3	g_2	g_2	37.5	0.0	y
3.6	g_3	g_2	g_2	39.5	0.0	n
3.7	g_2	g_2	g_2	0.0	0.0	y
3.8	g_2	g_2	g_2	0.0	0.0	y
3.9	g_2	g_2	g_2	0.0	0.0	y
4.0	g_2	g_2	g_2	0.0	0.0	y

A. Decision quality: regret against ground truth

Table III sweeps network stress and reports the true-state optimum alongside the two recommendations. The true worst interdiction is $A^\star_{\mathrm{true}} = g_2$ at every load. The sequential baseline selects the wrong unit g_3 over loads 3.3–3.6, whereas the joint estimator selects the correct g_2 from load 3.5 onward. Aggregated over the sweep, the joint estimator halves the mean interdiction regret against the true optimum (8.2 versus 17.9 MW), and its reserve estimate is 90 MW from the truth against the sequential estimate's 145 MW. Fig. 2(b) shows the joint decision boundary shifting to g_2 two load-steps earlier than the sequential one, seed-stable across seeds $\{1, 2, 3\}$ at 150 samples.

B. Why the change is narrow: the congestion mechanism

The change in the *selected* unit is confined to a narrow load band, and Fig. 4 explains why. At fixed stress, the minimum shed of the two competing interdictions crosses at a gas reserve of about 220 MW—below it g_2 is worse,

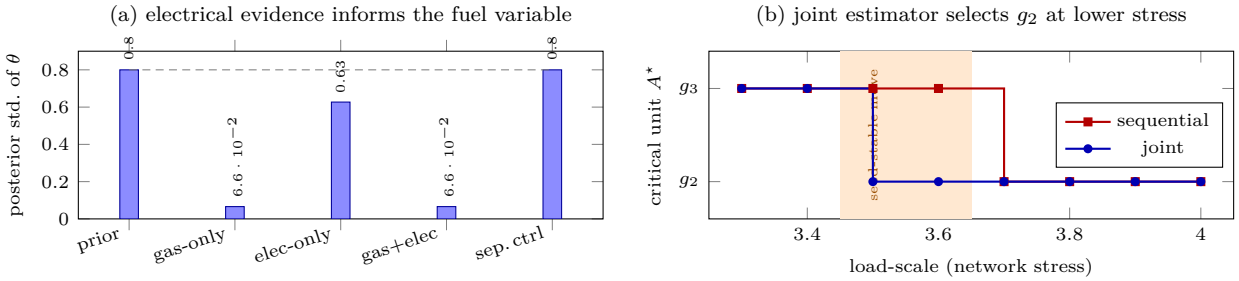


Fig. 2. Principal results, computed from the committed artifacts. **(a)** Posterior standard deviation of the fuel log-availability θ under different evidence. Remote electrical data alone (no fuel telemetry) reduces θ from its prior value (0.800) to 0.627 (21.7%); the separable control leaves it at 0.800, confirming that the coupling produces the update. **(b)** The joint estimator identifies generator g_2 as the critical interdiction two load-steps earlier than the sequential baseline; the shaded band indicates the region of disagreement, which is seed-stable at load 3.5.

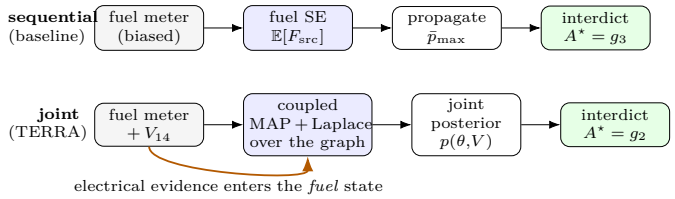


Fig. 3. Two decision pipelines over the same evidence. The *sequential* baseline estimates the fuel state from fuel telemetry only, propagates its mean into the generator capacity, and interdicts. The *joint* pipeline infers θ and the electrical state together through the coupled graph, so a remote electrical measurement corrects the fuel estimate before the decision. Only the joint path routes electrical data into the fuel state.

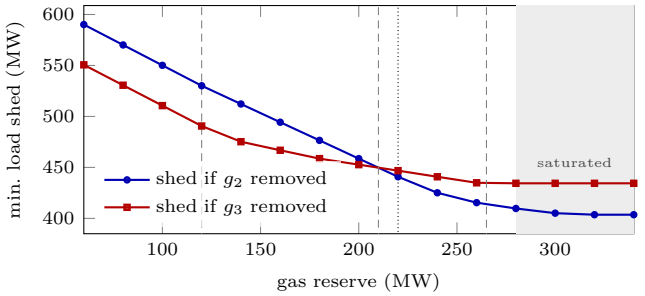


Fig. 4. Why the decision effect is narrow: the congestion mechanism (load-scale 3.6). The worst single-generator interdiction switches from g_2 to g_3 where the two shed curves cross, at a gas reserve of about 220 MW, and the shed *saturates* above ≈ 280 MW because additional reserve cannot reach load through the congested corridors. The true reserve (120 MW) and the joint estimate (210 MW) lie in the g_2 regime; only the sequential over-estimate (265 MW) crosses into the g_3 regime. The decision therefore differs only while the estimate pair straddles the crossover—a narrow band.

above it g_3—and the shed saturates beyond ≈ 280 MW because additional reserve cannot reach load through the congested corridors. The true reserve (120 MW) and the joint estimate (210 MW) lie in the g_2 regime, while the sequential over-estimate (265 MW) crosses into g_3. The selected interdiction therefore differs only while the estimate pair straddles the crossover, which occurs over a narrow load range on this capacity-rich network. The narrowness is a property of the transmission congestion, not of the inference: the reserve-estimate improvement is realized at every load, whereas the change in the selected unit is localized.

VII. Discussion and Limitations

The inference-level result (Section V) is robust: it is a property of the coupling, independent of the downstream decision, and stable across measurement conditions (Table II). The decision-level result (Section VI) has two parts that should be distinguished. The improvement in decision *quality*—a halving of mean regret and a reserve estimate 90 MW from truth—holds across the whole load sweep. The change in the *selected* interdiction is narrow, and Fig. 4 attributes this specifically to transmission congestion capping the usable reserve below the estimate-divergence range on this capacity-rich network. A network in which a single reserve is decisive over a wider range—for example one with a genuine islanding boundary—would widen the band; this is a direction for future work. The paper makes no claim that a fixed-scenario mixed-integer program is incapable of this in principle. The claim is at the level of capability: the engine performs cross-domain coupled inference directly from a declarative model, which a fixed-scenario, single-domain workflow does not.

VIII. Conclusion

Coupled multi-conservation graph inference can convert evidence in one conservation domain into a corrected decision variable in another. On the IEEE 14-bus network, conditioning the interdiction on a cross-domain posterior halves the mean regret against the true-state optimum and brings the reserve estimate 90 MW from truth. The change in the selected interdiction is confined to a narrow stress band, which a congestion mechanism explains rather than leaves as an anomaly. The construction—an equality injection that places the fuel variable inside an electrical residual (Proposition 1), with a separable control—its acceptance gate, and the supplementary analyses are reproducible from the committed artifacts, and the coupled model builder is provided as a tested engine component.

References

[1] S. M. Rinaldi, J. P. Peerenboom, and T. K. Kelly, "Identifying, understanding, and analyzing critical infrastructure interdependencies," *IEEE Control Syst. Mag.*, vol. 21, no. 6, pp. 11–25, Dec. 2001.

[2] J. Salmeron, K. Wood, and R. Baldick, "Analysis of electric grid security under terrorist threat," *IEEE Trans. Power Syst.*, vol. 19, no. 2, pp. 905–912, May 2004.

[3] D. Bienstock and A. Verma, "The N–k problem in power grids: New models, formulations, and numerical experiments," *SIAM J. Optim.*, vol. 20, no. 5, pp. 2352–2380, 2010.

[4] K. Sundar, C. Coffrin, H. Nagarajan, and R. Bent, "Probabilistic N–k failure-identification for power systems," *Networks*, vol. 71, no. 3, pp. 302–321, 2018.

[5] K. Sundar, A. Mastin, M. Garcia, R. Bent, and J.-P. Watson, "Exact and heuristic approaches for the stochastic N–k interdiction in power grids," *arXiv:2402.00217*, 2024.

[6] M. Geidl and G. Andersson, "Optimal power flow of multiple energy carriers," *IEEE Trans. Power Syst.*, vol. 22, no. 1, pp. 145–155, Feb. 2007.

[7] F. C. Schweppe and J. Wildes, "Power system static-state estimation, Part I: Exact model," *IEEE Trans. Power App. Syst.*, vol. PAS-89, no. 1, pp. 120–125, Jan. 1970.

[8] A. Abur and A. G. Expósito, *Power System State Estimation: Theory and Implementation*. New York, NY, USA: Marcel Dekker, 2004.

[9] C. M. Bishop, *Pattern Recognition and Machine Learning*. New York, NY, USA: Springer, 2006.

[10] R. D. Zimmerman, C. E. Murillo-Sánchez, and R. J. Thomas, "MATPOWER: Steady-state operations, planning, and analysis tools for power systems research and education," *IEEE Trans. Power Syst.*, vol. 26, no. 1, pp. 12–19, Feb. 2011.